

Contactless Measurement of the Heat of Fusion of Reactive Metallic Alloys¹

R. K. Wunderlich^{2,3}, Ch. Ettl² and H.-J. Fecht²

¹ Paper presented at the Fourteenth Symposium on Thermophysical Properties,
June 25-30, 2000, Boulder, Colorado, U.S.A.

² Abteilung Werkstoffe der Elektrotechnik, Universität Ulm, Albert-Einstein-Allee 47,
D-89081 Ulm

³ Author to whom correspondence should be addressed.

ABSTRACT

A new non-contact technique for the measurement of the heat of fusion of reactive metallic alloys in an electromagnetic levitation device is described. The technique is based on the evaluation of the power balance between radio frequency induction heating and radiative heat loss in transient heating and cooling experiments. Non-contact ac-calorimetry is applied for calibration of the electromagnetic coupling between the specimen and the rf-fields as well as for the evaluation of the total hemispherical emissivity from heat capacity and radiative relaxation time measurement. The technique has been applied to Zr-based metallic glass forming alloys with the containerless electromagnetic processing device TEMPUS under conditions of reduced gravity as part of a program for the investigation of the thermodynamic functions of metallic glass forming alloys in the stable and undercooled melt.

1. INTRODUCTION

The heat of fusion, ΔH_f , is a critical input parameter for the evaluation of the thermodynamic functions of the liquid phase as well as of considerable importance in the modeling of industrial solidification and casting processes. However, for many metallic alloys application of standard methods of enthalpy measurement such as differential thermal analysis (DTA) become quite difficult due to the ubiquitous presence of container reactions at elevated temperatures. Drop calorimetry offers a different approach. Quantitative determination of ΔH_f requires detailed account of the radiative heat loss during the free fall and cooling of the specimen. Furthermore, many specimens in particular, metallic glass forming alloys solidify into metastable phases making difficult the determination of the transformation enthalpy with respect to well characterized equilibrium phases. Pulse heating techniques have been applied successfully for pure metals¹ with radiative heat loss determined from the total hemispherical emissivity.

Here we describe an entirely contactless method for the measurement of the heat of fusion based on electromagnetic levitation and pyrometric temperature measurement. Electromagnetic levitation has found increased application for the investigation of the thermophysical properties of liquid metallic alloys². Similarly to the pulse heating technique the method is based on transient heating or cooling experiments, albeit on a much longer timescale, and the quantitative evaluation of the power balance between inductive radio frequency (rf) heating and radiative heat loss. Non-contact calorimetry³ is essential to the technique providing calibration of the electromagnetic power input^{4,5} as well as evaluation of the total hemispherical emissivity from measurement of the specific heat capacity and radiative relaxation time.

The technique grew out of a program for investigation of the thermodynamic functions of metallic glass forming alloys in the undercooled liquid and was applied to a series of binary and multicomponent Zr-based alloys in two spacelab experiments with the electromagnetic containerless processing device TEMPUS⁶.

2. CONTACTLESS ENTHALPY DETERMINATION

2.1 General Concept

A metallic specimen is positioned in an electromagnetic levitation device by a positioning field P_P (the positioner) and heated by a heating field P_H (the heater). The two fields have different frequencies allowing to separate the total rf-heating power input, P_{in} , into $P_{in} = P_P + P_H$. Temperature control is achieved by changing the current of the the heater oscillating circuit, I_H . The specimen exhibits a temperature time profile, $T(t)$, as the result of a change in $I_H(t)$. The change in enthalpy between temperature $T_1(t_1)$ and $T_2(t_2)$ will be given by the power balance between P_{in} and heat loss, P_{out} :

$$\Delta H = \int_{t_1}^{t_2} [P_{in}(t) - P_{out}(t)] dt \quad (1)$$

Under UHV conditions P_{out} is purely radiative with $P_{out} = A \sigma \epsilon T_o^4$. A , ϵ and σ depict the surface area, the total hemispherical emissivity and the Stefan-Boltzmann constant respectively. The time dependence of P_{in} originates from $I_H(t)$, and from the temperature and/or time dependence of the radius, and the electrical resistivity, $R(T)$ and $\rho(T)$ respectively, which determine the electromagnetic coupling between the specimen and the rf-fields. The time dependence of P_{out} originates from the $T^4(t)$ dependence of radiative heat loss, from $R(T)$ and, the dependence of ϵ on resistivity and temperature as well as changes in ϵ caused by surface segregation or impurity dissolution. In general

ΔH contains specific heat and enthalpy contributions. For eutectic alloys $\Delta t_m = t_2 - t_1$ depicts the duration of the isothermal melting plateau.

2.2 Evaluation of Input Power

From basic electromagnetic theory the rf-power input to the specimen can be described in terms of coupling coefficients^{7,8} of the heater and positioner field, G_H and G_P respectively, and the currents in the heater and positioner oscillating circuit, I_H and I_P respectively:

$$P_{in} = G_H I_H^2 + G_P I_P^2 \quad (2)$$

In our previous work on non-contact ac-calorimetry^{9,10} we have demonstrated the evaluation of $G_H(T_C)$ from application of modulation calorimetry at a calibration temperature T_C with well known specific heat $C_P(T_C)$: I_H is sinusoidally modulated according to $I_H(t) = I_{H0} + I_\omega \sin(\omega t)$ resulting in an increase in average temperature, ΔT_{av} , and stationary modulation components ΔT_ω and $\Delta T_{2\omega}$. It was demonstrated that for metallic specimen in a wide range of temperature and sample size modulation frequencies can be found^{10,11} allowing to neglect the effect of finite thermal conductivity and radiative heat loss resulting in an isothermal temperature modulation. This condition is met if Biot number, Bi , specifying the rate of external heat loss to internal heat transfer satisfies $Bi \ll 1$ which is readily met for metallic specimen. Under these conditions:

$$\Delta T_\omega = G_H \frac{2 I_{H0} I_\omega}{C_P \omega} \quad (3)$$

$$\Delta T_{av} = G_H \frac{1}{2} I_\omega^2 \frac{\tau_1}{C_P} \quad (4)$$

with $\Delta T_{\omega}/T_o \ll 1$ and $\Delta T_{av}/T_o \ll 1$. T_o is the bias temperature corresponding to I_{Ho} and I_p . τ_1 depicts the external relation time for radiative heat loss which for $Bi \ll 1$ is:

$$\tau_1 = \frac{C_p}{4 A \sigma \varepsilon T_o^3} \quad (5)$$

τ_1 is easily obtained from the temperature decay to equilibrium following a small step function change in power input. For $Bi \ll 1$ this decay is purely exponential. Thus $G_H(T_c)$ is determined from measurement of ΔT_{ω} , $I_H(t)$ and $C_p(T_c)$.

G_p can be determined in two ways. First, from power balance at stationary temperature T_o we have $G_p I_p^2 = P_{out} - G_H I_{Ho}^2$. It is more convenient, to use Eq.(5) such that:

$$P_{out} = \frac{C_p T_c}{4 \tau_1} \quad (6)$$

not requiring explicit evaluation of ε while τ_1 can be measured with high accuracy.

Alternatively, Eq. (4) can be applied to a small change in the positioner current , ΔI_p :

$$\Delta T_{av} = G_p \Delta I_p (2I_p + \Delta I_p) \frac{\tau_1}{C_p} \quad (7)$$

allowing evaluation of G_p . The ratio G_H/G_p is purely geometrical and an instrument constant for specimens of the same dimensions. Thus G_p can be scaled in fixed proportion to G_H in the course of a phase transiton involving changes in R and ρ .

Scaling of $G_H(T_c)$ to the temperature range of interest and in the course of a phase transiton requires knowledge of $\rho(T)$ and $R(T)$ according to:

$$G_H = 3\pi R(T) \rho(T) F(x) L_H \quad (8)$$

$F(x)$ is a function of the characteristic length scale for rf-coupling, $x = R/\delta$, with δ the skin depth, $\delta = 5.33 \sqrt{\rho / f_H} \text{ cm}$ (ρ in $10^{-6} \Omega\text{cm}$ and the rf-frequency f_H in sec^{-1}). $F(x)$ has been evaluated and is available in closed form^{13,12}. For the range in resistivity typical for many liquid transition metal alloys, i.e $\rho \approx 140 \mu\Omega\text{cm}$, $F(x)$ is approximated with high accuracy by $F(x) = x - 1$. The main contribution to the change in $G_H(T)$ originates from the melting transition due to the change in resistivity and radius. The contactless determination of the specimen resistivity and of the rf-power input in the TEMPUS facility has been described by Lohöfer and Egrý¹³. $R(T)$ can be measured by a high resolution camera¹⁴.

2.3 Output Power

Under UHV conditions heat loss is purely radiative. In an actual experiment C_p and τ_1 measurements are performed at temperatures T_1 and T_2 in the pure phases to obtain $\epsilon(T_1)$ and $\epsilon(T_2)$. A linear extrapolation is applied in $\Delta T = T_2 - T_1$ containing the phase transition of interest. As compared to total radiance measurements, here $\epsilon(T_{1,2})$ is evaluated from the transient temperature response and thus not affected by effects of scattered light. Because the specimen is in close proximity to some reflecting surfaces such as the induction coils the reduction in radiative heat loss by the (small) fraction reflected back to the specimen is contained in the τ_1 measurement thus making $\epsilon(T)$ to an effective emissivity and including reflectivity effects in P_{out} . The extrapolation described here has its drawbacks in case of surface segregation or impurity dissolution. These can be overcome by using a total radiance pyrometer (bolometer) based e.g. on a pyroelectric detector. In this case detailed account of scattered light effects must be made as described by Cezairlyan¹⁵.

The analysis outlined above applies equally to melting and solidification. Differences arise in the relative contribution of P_H and P_{Pos} and P_{in} and P_{out} to the power balance. Melting is typically performed by application of a high power melt pulse reducing the relative contributions of P_{Pos} and P_{out} . Conversely, during solidification with reduced heater power the relative contribution of P_{Pos} and P_{out} is increased. Regarding evaluation of ΔH_f from the duration of a recalescence plateau the enthalpy necessary to heat the undercooled liquid from maximum undercooling to the eutectic or solidus temperature, i.e. $\Delta H_u = \Delta T_u C_p(av)$, has to be taken into account. $C_p(av)$ represents the average heat capacity in the undercooled melt in ΔT_u . It should be pointed out that all physical quantities required for the evaluation of ΔH can be obtained in one experimental setting.

3 EXPERIMENTAL SET UP

In TEMPUS, $R = 4$ mm specimen contained in an open cage holder were positioned in the center of a rf-quadrupole field (positioner) superimposed by a rf-dipole field (heater) with frequencies $f = 200$ kHz and 380 kHz, respectively. Temperature control was performed by adjusting the heater oscillating circuit voltage, U_H . I_H , U_H and the corresponding values for the positioner could be measured at a sampling rate of 10 Hz and 12 bit resolution.

Temperature was measured by a two channel 100 Hz sampling rate optical pyrometer operating in the wavelength range of $(1.8 - 2.8) \mu m$ and $(3.0 - 4.0) \mu m$. The pyrometer had a signal to noise ratio allowing measurement of temperature variations of < 0.1 K at a bias temperature of 1400 K. Pyrometry in TEMPUS is described in more detail by Hofmeister et al.¹⁶. The specimen shape was recorded with a high resolution

camera for measurement of the thermal expansion and the volume change on melting¹⁷. Processing was performed under ultrahigh vacuum.

4. ΔH_f EVALUATION

The alloy Zr-36 at.%Ni with eutectic temperature $T_e = 1283$ K shall serve as a specific example. ΔH is evaluated from the duration of the isothermal melting and

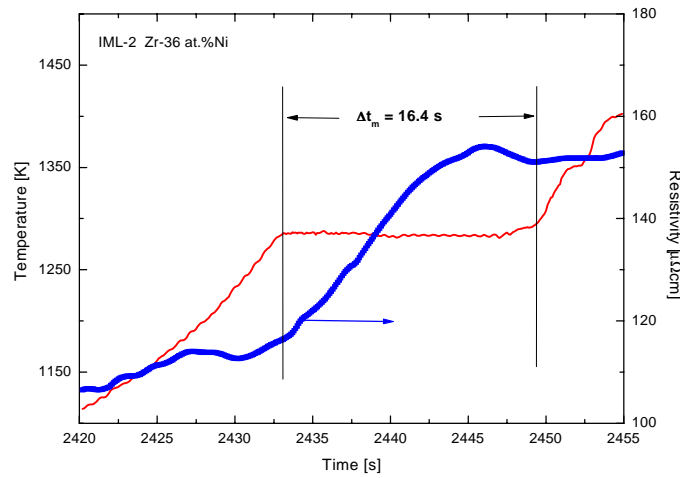


Fig. 1: Temperature- and resistivity-time profile for melting of a Zr-36 at.%Ni specimen. Left hand ordinate: temperature; right hand ordinate: resistivity, arrow attached to curve

solidification plateau with low undercooling shown in Fig.1 and 2, respectively. The rather long duration of the recalescence plateau as compared to melting, is caused by the residual heating effects of the positioning and heating fields. $G_H(T_c)$ was determined in the crystalline phase at $T_C = 1243$ K with $c_p(T_C) = 31.2$ J/Kmol determined by DSC. Modulation frequencies $\omega = 0.08$ and 0.10 Hz were determined to fall well within the

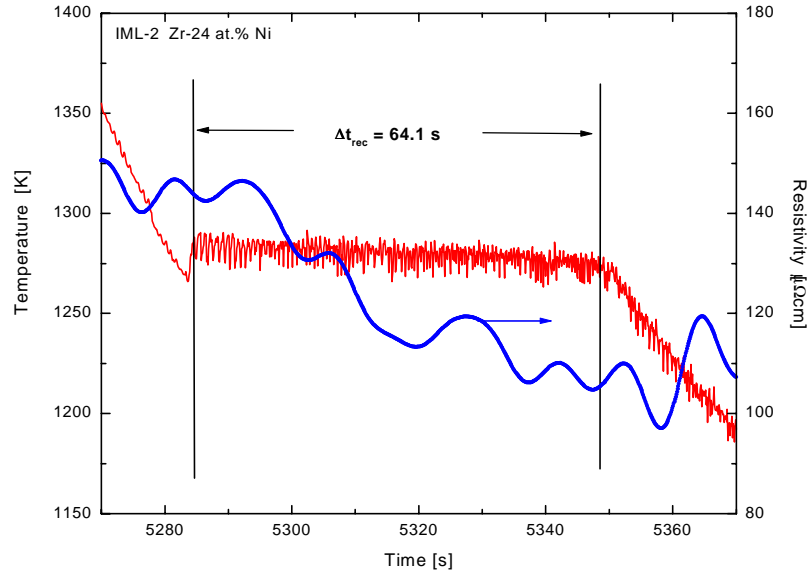


Fig.2: Temperature- and resistivity time profile of a cooling curve of Zr-36at%Ni specimen. Left hand ordinate: temperature; right hand ordinate: resistivity , arrow attached to curve. Δt_{rec} : duration of recalescence plateau 64.1 sec.

isothermal modulation regime. ΔT_{ω} was evaluated from Fourier analysis of the temperature response; typically $\Delta T_{\omega} \approx 6$ K. Fourier analysis of $I_H(t)$ provided $2I_{H0}I_{\omega}$. With these data we obtain $G_H(T_c) = 3.7$ Ohm. $G_H(T_c)$ obtained for $\omega = 0.08$ and 0.10 Hz agreed to better 1%.

$G_H/G_P = 25.6$ was obtained from $P_{\text{out}}(T_c) = 7.4$ W with $\tau_1(T_c) = 29.1$ s and application of Eq.(6). From Eq.(5) we obtain $\epsilon(T_c) = 0.29$ which was scaled according¹⁸ to $\epsilon \propto (\rho T)^{1/2}$ to obtain the total hemispherical emissivity in the crystalline phase at the eutectic temperature as $\epsilon^x(T_e) = 0.31$. From modulation calorimetry and τ_1 measurement at $T_e + 10$ K we obtained $\epsilon^l(T_e) = 0.32$ in good agreement with the $(\rho T)^{1/2}$ scaling. The volume change on melting was obtained as $\Delta V/V = 0.028$.

Considering the resistivity shown in Fig. 1 there is a transient regime $\Delta t_{tr} \approx 2/3 \Delta t_m$ until $\rho(t) \approx \text{const.}$ reflecting the duration of the melting process within the skin depth. A similar effect is observed for solidification as shown in Fig.2. The larger scatter in $\rho(t)$ for the recalescence plateau is due to the much reduced heater current resulting in a decreased signal to noise ratio in the measurement of U_H and I_H . For melting with $\Delta t_m \leq 20$ s typical values for the power balance are $P_H = 35$ W, $P_P = 2$ W while $P_{out} = 9$ W.

The data $T(t)$, $I_H(t)$, $U_H(t)$ and $I_P(t)$ obtained directly from the experiment recording in digital form are fed into an algorithm calculating $\rho(t)$ and performing the integration of Eq.1. The $\varepsilon(t)$, $R(t)$ and t_1, t_2 the beginning and end of the melting or solidification intervall are read from a specimen data file making ΔH evaluation to a routine operation.

A compilation of ΔH obtained from a series of meltpulses (●) with different Δt_m is shown in Fig.3. While the data converge for $\Delta t_m < 20$ s the apparent decrease of ΔH for increased Δt_m i.e. with the application of smaller heater current pulses is caused by a slow propagation of the melting front from the equatorial plane where power coupling is maximum to the polar position where temperature is measured. The data points marked (▲) were obtained from evaluation of recalescence plateaus with undercooling $\Delta T_u \leq 10$ K after correcting for the enthalpy required to heat the undercooled liquid to T_e . The specific heat was taken as that of the liquid⁵ at T_e with $c_p^1(T_e) = 44.6$ J/K mol. These data points were inserted into the figure without reference to the abscissa.

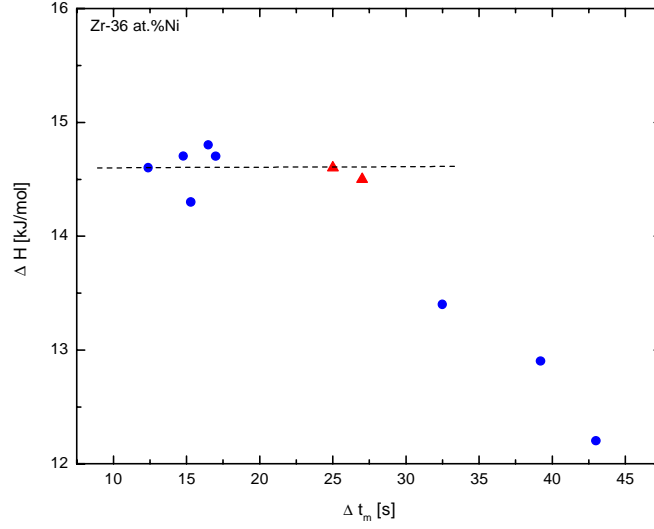


Fig. 3: Transformation enthalpy of Zr-36at%Ni as function of the duration of the melting plateau (●). Data points (▲) indicate values obtained from evaluation of recalescence plateaus following low undercooling, inserted into the figure without reference to the abscissa.

Application of the method to an alloy with an extended melting range is demonstrated in Fig. 4 for the alloy Zr-23 at.%Co with very near eutectic composition. The solidus temperature, $T_s = 1205$ K, is obtained from the onset of the melting plateau. The liquidus temperature, $T_l = 1258$ K, is identified from the change in slope of the heating curve indicating an increase in dT/dt after the specimen is completely molten. This is also reflected by the behavior of $\rho(t)$ with $\rho(t) \approx \text{const.}$ for $T \geq T_l$. Integration of Eq.1 between T_s and T_l results in a total enthalpy change $\Delta H = 13.4$ kJ/mol. This value has to be reduced by the contribution of the liquid specific heat requiring knowledge of the fraction solid as function of $T(t)$. First, from modulation calorimetry we obtain $c_p^l(1305 \text{ K}) = 43.3$ J/K mol. We assume $c_p^l(T) = \text{const.}$ and use the time dependence of

$\rho(t)$ in the two phase region to scale the fraction solid from 1 to 0 between T_s and T_l . We thus obtain a liquid specific heat contribution of 1.15 kJ/mol to the measured change in enthalpy resulting in $\Delta H_f = 12.3$ kJ/mol. Determination of the fraction solid from $\rho(t)$ is a more serious approximation because the rf-field probes only the skin depth of $\delta \approx 1$ mm. However, as soon as there is some significant liquid fraction electromagnetic will

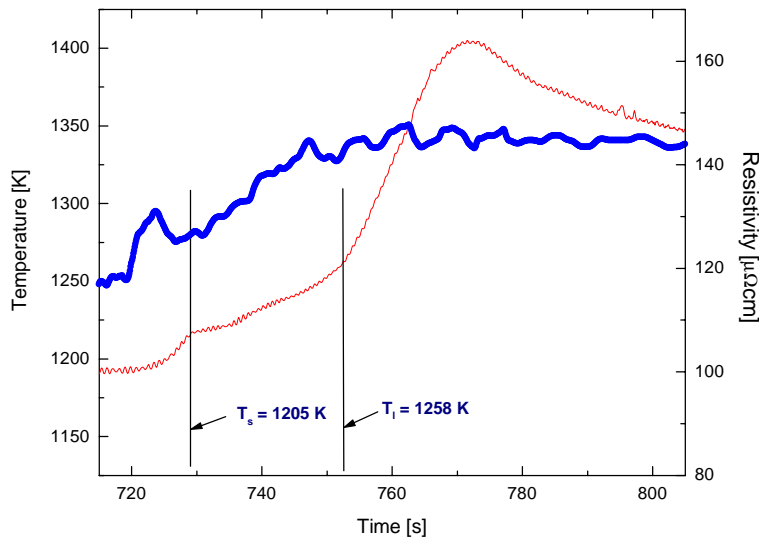


Fig. 4: Temperature- and resistivity-time profile for melting of Zr-23at%Co. Left hand ordinate: temperature; right hand ordinate: resistivity. Horizontal lines: two phase region. Solidus $T_s = 1205$ K, liquidus $T_l = 1254$ K .

average the solid fraction over the entire volume. For an improvement it has recently been shown¹⁹ that application of non contact ac-calorimetry in the two phase region at constant average temperature provides a very sensitive determination of the fraction solid as well as a very accurate determination of T_l . If rf-power is abundant the rf-frequency may be lowered to increase the directly probed volume fraction.

Identification of the measured ΔH the enthalpy of fusion requires consideration of the phase equilibria present at the onset of the melt pulse or after recalescence. Regarding melting, specimens were annealed for prolonged periods of time at $T_e - 100$ K before application of a melting pulse. Specific heat measurements and x-ray analysis as function of annealing time showed that these times were sufficient to establish crystalline phase equilibrium. For Zr-36 at.%Ni and Zr-24 at.%Fe there was very good agreement between ΔH obtained from melting and recalescence plateaus. For Zr-23 at.%Co ΔH evaluated from melting was consistently larger by 1.1 kJ/mol than ΔH evaluated from solidification. This discrepancy is most likely due to the presence of the metastable cubic Zr_2Co phase revealed by X-ray analysis of rapidly cooled ingots.

5. RESULTS AND DISCUSSION

Table 1 summarizes ΔH_f for the binary Zr alloys processed in the experiments and the thermophysical properties relevant for the evaluation. The change in specific heat capacity between liquid and solid phase at the eutectic temperature, Δc_p^{lx} is listed in column two. For the Zr-24 at.%Fe alloy there is comparison available with a determination by drop calorimetry²⁰ as $\Delta H_f = 9.3 \text{ kJ mol}^{-1}$ lending support to the accuracy of the method presented here. The ΔH_f values in Tab.1 present averages obtained from melting with $\Delta t_m < 20$ s. For Zr-36 at.%Ni the average includes also data obtained from recalescence plateaus following low undercooling. As shown in Fig.3 the reproducibility of ΔH_f such obtained is $< 2\%$. The good agreement between ΔH_f values obtained from melting and solidification with very different contributions of P_{in} and P_{out} to the power balance demonstrates the consistency of the approach and the accuracy in the evaluation of the coupling constants and the total hemispherical emissivity. The

Tab. 1: Thermophysical properties at T_e in the liquid (l) and crystalline phase (x) of Zr-based binary alloys. ΔH_f heat of fusion in kJmol^{-1} ; $\Delta c_p^{l,x}$: specific heat difference at T_e in $\text{JK}^{-1}\text{mol}^{-1}$; ρ resistivity in $\mu\Omega\text{cm}$ of liquid and solid phase respectively; ϵ^l : total hemispherical emissivity. For the alloy $\text{Zr}_{77}\text{Co}_{23}$ l and x refer to T_l and T_s respectively.

Alloy	ΔH_f	$\Delta c_p^{l,x}$	ρ^l	ρ^x	ϵ^l	ϵ^x
$\text{Zr}_{64}\text{Ni}_{36}$ $T_e = 1283 \text{ K}$	14.6	12.2	152	138	0.32	0.31
$\text{Zr}_{76}\text{Ni}_{24}$ $T_e = 1233 \text{ K}$	11.0	8.9	138	116	0.28	0.26
$\text{Zr}_{76}\text{Fe}_{24}$ $T_e = 1208 \text{ K}$	9.5	7.4	128	112	0.26	0.24
$\text{Zr}_{77}\text{Co}_{23}$ $T_l = 1254 \text{ K}$	12.3	12.0	141	122	0.31	0.29

validity of the approach for the emissivity evaluation is further supported by the good correlation between ρ^l and ϵ^l for all alloys investigated.

The absolute accuracy depends on whether ΔH_f is evaluated from melting or solidification. Focussing on the former, ΔT_ω and I_H can be determined with an accuracy $\leq 2\%$. Thus the accuracy of $G_H(T_c)$ is determined largely by the accuracy of $c_p(T_c)$ as obtained from conventional DSC. For scaling of $G_H(T_c)$ the absolute accuracy of the resistivity may be conservatively estimated as only $\leq 10\%$. However the relative change

in $\rho(T)$ can be obtained with much higher accuracy. As such, the accuracy of $G_H(T_e)$ is estimated as $\leq 4\%$. According to the numbers given above during melting P_{out} contributes typically 30% to the power balance. With a conservative error of 5 % in ϵ the over all accuracy of ΔH_f evaluated from melting is obtained as $< 6\%$. This value is considered as a true upper limit pertaining to a specific experimental set up. It can be further reduced with increased experimental effort.

6. CONCLUSION

We have presented a new contactless method for the determination of the heat of fusion of reactive metallic alloys based on induction heating of electromagnetically levitated specimens and pyrometric temperature measurement. Non-contact calorimetry was essential for calibration of the heating power input as well as evaluation of the total hemispherical emissivity in combination with the measurement of the external radiative relaxation time. With these input values, and the analysis of video recordings for the change in specific volume during the melting transition the power balance between electromagnetic input power and radiative heat loss during melting or solidification was evaluated. The experiments have been performed with the containerless electromagnetic processing device TEMPUS in two spacelab missions. Adaption of this method to 1-g conditions may circumvent problems encountered in a precise determination of the enthalpy of fusion of highly reactive metallic alloys.

ACKNOWLEDGEMENTS

We gratefully acknowledge support by Dr. G. Lohöfer from the German Space Establishment (DLR) in the resistivity and by Dr. B. Damaschke (University of Göttingen). Support by the German space agency DLR (DARA Grant No. 50 WM 94-31-4) is gratefully acknowledged.

REFERENCES

- ¹ A. Cezairliyan and J.L. McLure, Int. J. Thermophys. **8**: 577 (1987)
- ² D. M. Herlach, R. F. Cochrane, I. Egry, H. -J. Fecht, and A. L. Greer, Int. Mat. Rev. **38**, 273 (1993)
- ³ H. -J. Fecht and W. L. Johnson, Rev. Sci. Instr. **62**, 1299 (1991)
- ⁴ R. K. Wunderlich and H.-J. Fecht, Int. J. Thermophys. **17**, 1203 (1996)
- ⁵ R. K. Wunderlich, D. S. Lee, W. L. Johnson, and H. -J. Fecht, Phys. Rev. **B55**, 16 (1997)
- ⁶ I. Egry, J. Jpn. Soc. Microgravity Appl., **15**, 215 (1998)
- ⁷ G. Lohöfer, SIAM J. Appl. Math. **49**, 567 (1989)
- ⁸ B.Q. Li, Int. J. Eng. Sci. **31**, 201 (1993)
- ⁹ R. K. Wunderlich, D. S. Lee, W. L. Johnson, and H. -J. Fecht, Phys. Rev. **B 55**, 16 (1997)
- ¹⁰ R. K. Wunderlich and H.-J. Fecht, Int. J. Thermophys. **17**, 1203, (1996)
- ¹¹ R. K. Wunderlich, R. Willnecker and H.-J. Fecht, Appl. Phys. Lett. **62**, 3111 (1993)
- ¹² G. Lohöfer, Int. J. Eng. Sci. **32**, 107 (1994)
- ¹³ G. Lohöfer and I. Egry, Solidification 99, 65 (TMS Warrendale 1999, eds. W. H. Hofmeister, J. R. Rogers, N. W. Sing, S. P. March and P. W. Vorhees)
- ¹⁴ B. Damaschke, D. Oelgeschläger, J. Ehrich, E. Dietzsch and K. Samwer, Rev. Sci. Instr. **69**, 2110 (1998)
- ¹⁵ A. Cezairliyan, Compendium of Thermophysical Property Measurement, eds. K. D. Maglic, A. Cezairliyan, V. E. Peletsky, Plenum Press New York 1992, pp 483
- ¹⁶ W. H. Hofmeister, R. J. Bayuzik and S. Kishnan, Space Processing of Materials, ed. N. Ramachandran, Proc. SPIE, vol **2809**, 1996 pp.288

¹⁷ B. Damaschke and K. Samwer, Appl. Phys. Lett.**75**, 2220 (1999)

¹⁸ A. J. Sievers, J. Opt. Soc. Am.**68** (1978) 1505 – 1516

¹⁹ R. K. Wunderlich, Ch. Ettl, A. Sagel, H.-J. Fecht., S.L. W.L. Glade Johnson,
Proceedings TMS Annual Meeting 2000, Nashville (TMS Warrendale)

²⁰ M. Rösner-Kuhn, Technische Universität Berlin, private communication